The M-Meter: A Simple Airborne Hydrometeor Measurement Instrument

ANDREW DETWILER

Institute of Atmospheric Sciences, South Dakota School of Mines and Technology, Rapid City, South Dakota

HILLYER G. NORMENT

Atmospheric Science Associates, Concord, Massachusetts

14 October 1997 and 7 December 1998

ABSTRACT

The M-meter is designed to measure total mass concentration of hydrometeors from aircraft aloft. Its essence is a free-rotating, vaned disk with face normal to the freestream; rotation is driven by airflow through the vanes. Hydrometeors collected on the disk surface are expelled by being flung tangentially from its periphery. This expulsion causes a reduction of equilibrium rotation rate that is proportional to freestream hydrometeor mass concentration.

A prototype was carried under the wing of a research airplane as it probed precipitating clouds at levels from just above to just below the melting layer. M-meter measurements of hydrometeor mass concentrations are demonstrated to be in qualitative agreement with independent measurements.

This unique, simple, rugged instrument with high sampling volume probably can be refined to provide accurate in situ measurement of cloud plus precipitation water mass—a capability sorely needed. It warrants additional research and development, which is not planned by those involved at present. This note is for the purpose of stimulating further interest in this promising concept.

1. Introduction

There have been many instruments developed to measure concentrations of hydrometeors, each of which is a compromise among cost, weight, power consumption, hydrometeor size range to which it responds, volume sampling rate, resolution, precision, and ease of use and data analysis. We describe a prototype M-meter that was conceived and built by Vernon G. Plank[1] (Plank 1986) of the Phillips Laboratory, U.S. Air Force, to measure total mass concentration of all types and sizes of hydrometeors, and we present some flight test results. The M-meter was designed specifically for use in a mixed-phase environment. This instrument has many desirable characteristics, including modest cost, negligible power consumption, mechanical and electrical simplicity, response to hydrometeors ranging in size from a few micrometers to centimeters, and a relatively high volume sampling rate. No other instrument in current use can claim more than one or two of these virtues. Moreover, with further development, M-meter accuracy probably can be made competitive with and/or better than that of other available instruments.

2. Description of the prototype

The essential element of the prototype M-meter is a free-rotating, titanium disk of radius 3 cm and weight 37 g mounted with face normal to the freestream. The disk surface is machined such that it has 30 canted vanes on an annulus between radii 2 and 3 cm (Fig. 1). Airflow through these vanes drives rotation. In clear air at true airspeed of about 82 m s^{-1}, rotation rate is about 2450 radians s^{-1} (23 400 rpm). During in-cloud operation, hydrometeors collected on the disk are expelled tangentially from its periphery; this extracts angular momentum from the disk and causes a decrease in equilibrium (i.e., steady state) rotation rate that is proportional to freestream hydrometeor mass concentration. Response of the spinning disk to transient change in airspeed and hydrometeor concentration is fast enough that rotation may be taken to be approximately steady state, not only in clear air, but in cloud as well.

The complete prototype is shown in Fig. 2. The nonrotating, parabolic cone ahead of the disk directs a smooth flow of air and hydrometeors to the vaned portion of the disk surface (between radii 2 and 3 cm). The nonrotating ring assembly (with triangular cross section) just forward of the outer edge of the disk contains a heater to de-ice the vanes, as does the cone, but de-

[1] Deceased; U.S. Patent 4,815,314, Particulate Mass Measuring Apparatus.

Corresponding author address: Dr. Andrew Detwiler, IAS/SDSMT, 501 E. St. Joseph Street, Rapid City, SD 57701-3995.
E-mail: andy@ias.sdsmt.edu

FIG. 1. Front view of M-meter disk and flow-directing center cone.

icing was not used during the field tests described here. The nonrotating housing behind the disk contains a photodetector and a simple electronics package. The photodetector registers passage of marks on the back side of the spinning disk, and these data, which constitute the only output of the instrument and from which rotation rate is calculated, are transmitted to the central data acquisition system. The prototype is about the size of a hand-held flashlight.

3. Operation equation

We use angular momentum conservation to derive an equation to calculate hydrometeor mass concentration from disk rotation rate. Angular momentum, L, of the rotating disk is

$$L = \omega m r_g^2, \tag{1}$$

where ω is rotation rate, m is disk mass, and r_g is its radius of gyration. Conservation of angular momentum requires that change in L be accompanied by application of a torque, T, such that $dL/dt = T$, and we have by differentiation of (1):

$$r_g^2\left(m\frac{d\omega}{dt} + \omega\frac{dm}{dt}\right) = T = T_P - T_R - T_X, \tag{2}$$

where T_P is dynamic air pressure torque on the vanes, which acts to rotate the disk; T_R is reaction torque caused by expulsion of hydrometeors from the outer periphery of the disk, which acts to reduce its rotation; and T_X are miscellaneous torques (for example, boundary layer friction and bearing friction torques), which are of uncertain significance. They are ignored hereafter but need to be evaluated by laboratory measurement. We show

FIG. 2. M-meter prototype in operating configuration. It is 6 cm in diameter, 20 cm long, and has a mass of 1.4 kg.

elsewhere (Norment 1982) that for the straight, canted vanes of the prototype, dynamic air pressure torque on the disk vanes has the form

$$T_P = \frac{1}{2}\rho V^2 r_2^3(a + b\Omega + c\Omega^2), \tag{3}$$

where ρ is air density, V is freestream airspeed, r_2 is outer radius of the disk (3 cm), $\Omega = \Delta r\omega/(2V)$ is a dimensionless rotation rate that is approximately constant during level flight in clear air, $\Delta r = r_2 - r_1$, and r_1 is the inner radius of the vaned surface annulus (2 cm). Dimensionless parameters a, b, and c are complex functions of vane geometry and local airflow between the vanes; while accurate values for them are not known, they are treated here as constants since, after initial start-up, the disk rotates essentially at its clear-air equilibrium rate, deviating only slightly from this even when in cloud (i.e., $T_R \ll T_P$). Define Ω_a to be nondimensional rotation rate under steady-state, clear-air conditions. Steady-state, clear-air rotation requires that

$$T_P = 0 = \frac{1}{2}\rho V^2 r_2^3(a + b\Omega_a + c\Omega_a^2), \tag{4}$$

and subtraction of (4) from (3) gives

$$T_P = -\frac{1}{2}\rho V^2 r_2^3(\Omega_a - \Omega)[b + c(\Omega_a + \Omega)].$$

Since there is only slight difference between in-cloud and clear-air rotation rates, $\Omega + \Omega_a \approx 2\Omega_a$, and $b + 2c\Omega_a$ can be approximated to be a constant, $-K$. [Also, from (4) note that $b + 2\Omega_a = -\sqrt{b^2 - 4ac}$. Thus our assumption that $b + 2\Omega_a \approx$ constant is consistent with our assumption that parameters a, b, and c are approximate constants.] With these substitutions we arrive at our final expression for dynamic air pressure torque

$$T_P \approx \frac{K}{2}\rho V^2 r_2^3(\Omega_a - \Omega). \tag{5}$$

To obtain the reaction torque, consider a parcel of water of mass Δm_w that is expelled from the outer periphery of the disk with tangential speed ωr_2. It carries with it a tangential momentum increment $\Delta m_w \omega r_2$, and in accord with the law of conservation of angular mo-

mentum and Newton's third law of motion, a reaction of equal magnitude and opposite direction must be felt by the disk. If expulsion occurs over a time interval Δt, the result is a tangential force, $\Delta m_w \omega r_2/\Delta t$, on the disk that acts to oppose its rotation. Since this force acts at distance r_2 from the rotation axis, it represents a torque, $\Delta m_w \omega r_2^2/\Delta t$. Summing around the disk periphery, and replacing deltas with differentials, we obtain the reaction torque

$$T_R = \omega r_2^2 \left.\frac{dm}{dt}\right|_{\text{loss}}. \tag{6}$$

We assume steady-state rotation of the disk, so that rate of loss of water carried by the disk is equal to its rate of gain, which is given by the standard accretion equation

$$\left.\frac{dm}{dt}\right|_{\text{loss}} = \left.\frac{dm}{dt}\right|_{\text{gain}} = \pi r_2^2 EMV, \tag{7}$$

where E is collection efficiency of the M-meter for hydrometeors and M is mass concentration of hydrometeors in the freestream. Substitution of (7) into (6) gives an expression for reaction torque in terms of M:

$$T_R = \pi r_2^4 EVM\omega. \tag{8}$$

Under steady-state conditions $d\omega/dt = dm/dt = 0$ so that the left side of (2) is zero. Substituting (5) and (8) for T_P and T_R in the right side of (2), and setting the left side to zero, we get

$$\pi r_2^4 EVM\omega \approx \frac{K}{2}\rho V^2 r_2^3(\Omega_a - \Omega),$$

which we solve for M, using the definition of Ω_a, to obtain our operation equation for the prototype M-meter:

$$M \approx \frac{K}{4\pi E}\frac{\Delta r}{r_2}\rho\left(\frac{\Omega_a - \Omega}{\Omega}\right) \approx \frac{K}{12\pi}\rho\left(\frac{\Omega_a - \Omega}{\Omega}\right), \tag{9}$$

where we have taken $E \approx 1$ (Norment 1982).

The apparent simplicity of (9) is deceptive. The equation applies to measurements of ω and V at an in-cloud point, from which Ω is calculated for that point. Raw disk rotation rate, ω, is measured with high accuracy by the prototype M-meter, and provided that V is also measured accurately in the same airspace, Ω can be obtained with high accuracy. To obtain M, this Ω is subtracted from Ω_a, which applies to a hypothetical measurement taken at the same time and point (or under identical conditions) in the absence of cloud. Such an Ω_a cannot be measured locally, so we must make do with an estimate; and since our result depends on the small difference $\Omega_a - \Omega$, the estimate must be highly accurate. Ramifications of this problem are discussed in section 4b. In addition, the parameter K appears not to be a true constant for the prototype. (It is important to note that for properly designed curved disk vanes, for which the operation equation is somewhat different, Ω_a and K are true constants, related to instrument design specifications, instead of inaccessible, variable parameters. Their values can be determined easily by both theory and measurement, so that their determination should not be a problem for refined versions of the M-meter.)

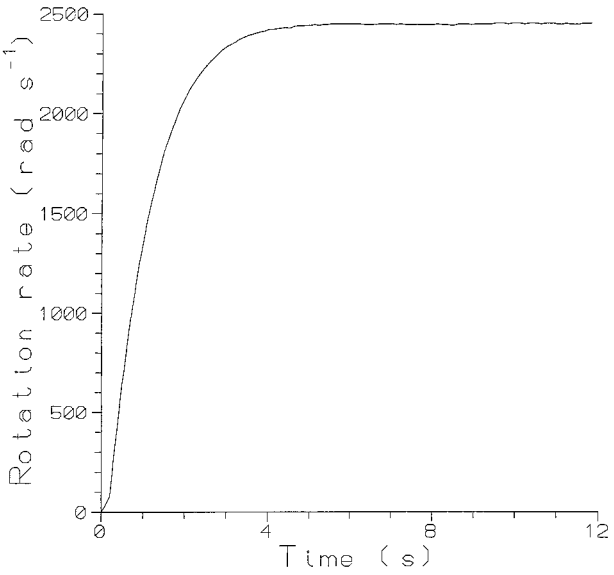

FIG. 3. M-meter disk spin-up rotation rate vs time following release of a brake during constant speed (82 m s^{-1}), level flight.

Response time of the M-meter to changing airflow is critical. Reaction must be fast enough that in-cloud disk rotation lag below its clear-air rate represents effects of hydrometeors, rather than effects of sluggish response to changing airflow (i.e., turbulence). Results of two studies, one experimental, the other theoretical, are presented to show that the response is sufficiently fast. In the experimental study, the prototype M-meter was flown at constant speed (82 m s^{-1}), altitude, and heading with the disk held motionless; then the disk brake was suddenly released to let the disk spin up to equilibrium. Approach to equilibrium was exponential, as shown in Fig. 3, with a time constant of $\sim$1.2 s.

An equation for calculation of nonequilibrium M-meter disk rotation (details are too extensive to be included here) was used for the theoretical study. Equation parameters obtained in the field were used (section 4b). In the study, steady-state clear-air rotation was interrupted by abrupt, continuous (sine function) surges in freestream air speed. These surges were from an initial freestream speed of 80 m s^{-1} up to a final freestream speed of 82 m s^{-1}, and occurred over time intervals Δt ranging from 3 to 30 s. (Freestream speed fluctuations of $\sim$2.5% over time intervals from 3 to 30 s are more or less typical of those encountered in observed data, as indicated in Figs. 4b and 6g.) To show speed of recovery of the instrument, we use the ratio $\omega_{\Delta t}/\omega_a$, where $\omega_{\Delta t}$ is the calculated disk rotation rate at the end

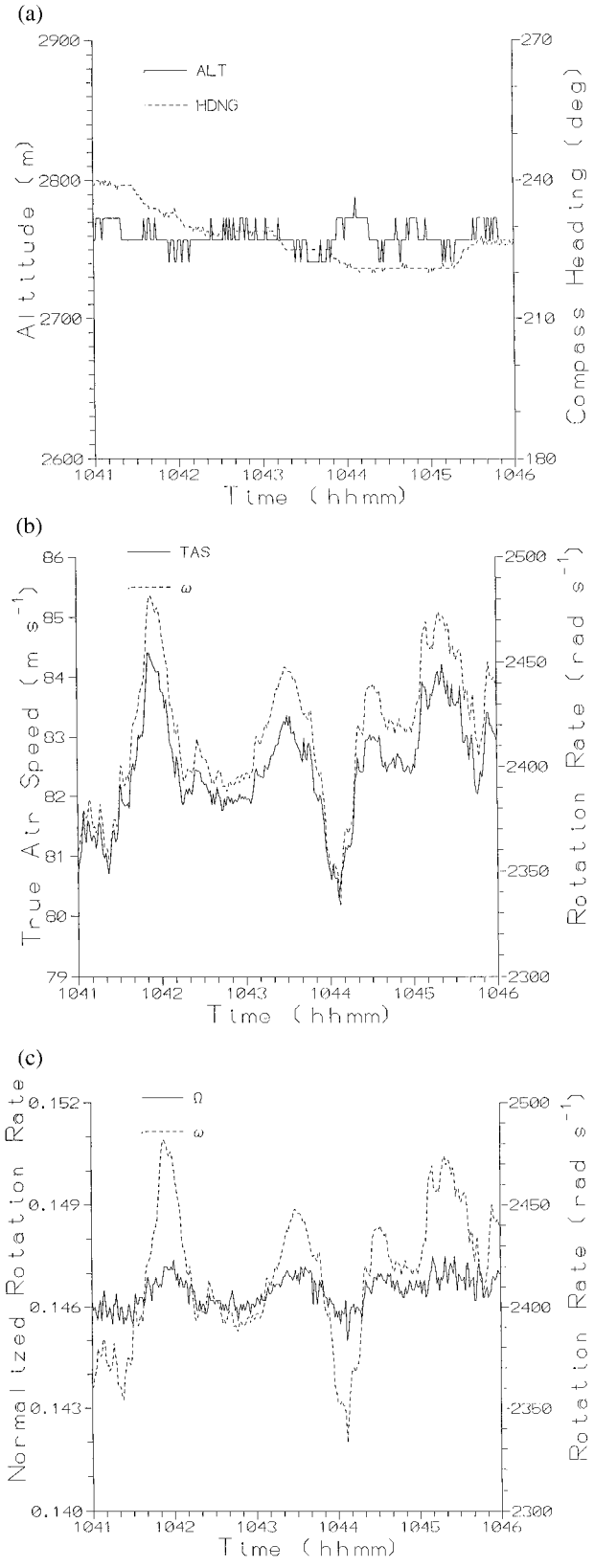

FIG. 4. (a) Altitude and compass heading vs time for a 5-min interval of level flight just prior to cloud penetration. (b) Airspeed V and M-meter disk rotation rate ω vs time for the flight interval shown in (a). Ordinate value ranges are roughly proportional in magnitude, that is, $(V_{max} - V_{min})/[(V_{max} + V_{min})/2] \approx (\omega_{max} - \omega_{min})/[(\omega_{max} + \omega_{min})/2]$, so that the data can be compared visually as shown. (c) M-meter disk rotation rate ω and normalized M-meter disk rotation rate Ω vs time for the flight interval shown in (a). Ordinate value ranges are roughly proportional in magnitude, that is, $(\omega_{max} - \omega_{min})/[(\omega_{max} + \omega_{min})/2] \approx (\Omega_{max} - \Omega_{min})/[(\Omega_{max} + \Omega_{min})/2]$, so that the data can be compared visually as shown.

TABLE 1. Theoretical sensitivity of the M-Meter to a surge in freestream airspeed.

V, ΔV (m s^{-1})	Δt (sec)	$\omega_{\Delta t}/\omega_a$	M_{con} (g m^{-3})
80, 2	3	0.983	0.456
	5	0.9975	0.066
	10	0.9998	0.005
	30	1.000	0

of a surge of duration Δt, and ω_a is the equilibrium disk rotation rate at the new freestream airspeed of 82 m s^{-1}. Equation (9) can be used directly to calculate ''lag contamination'' water content, M_{con}, from the difference between ω_a and $\omega_{\Delta t}$. Results are shown in Table 1.

Table 1 results indicate that an increase in airspeed of 2.5% within 3 s would cause the M-meter to register spurious M of about 0.5 g m^{-3}. If the same speed change were to occur over 5 s, the spurious M would be only about 0.07 g m^{-3}. Conversely, airspeed decrease of this amount over similar time intervals would result in negative M of similar magnitudes. During the flight segments examined below, changes in V of 2.5% rarely occurred over intervals of less than 5 s.

The measured time constant of 1.2 s, the theoretical results in Table 1, and visual comparison of air speed and disk rotation curves in Fig. 4b all indicate adequately fast disk rotation response to changing air speed. In addition, we have found that use of the nonequilibrium operation equation to calculate M from field data does not yield significant improvement of results over those obtained from (9). Thus, we conclude that our assumption of equilibrium operation of the M-meter is warranted, and also that M-meter M results should not be compromised by sluggish reaction to turbulence.

4. Field tests of the prototype

a. Introduction

The prototype M-meter was field tested, on a low-priority, piggyback status, in the spring of 1986 during an Air Force Geophysics Laboratory melting layer microphysics study (Davis and Lawson 1987). Conditions for its evaluation were far from optimal. It was mounted on a wingtip pylon carried by the Particle Measuring Systems (PMS) Beechcraft Baron airplane operated by Colorado International Corporation, along with a PMS

Forward Scattering Spectrometer Probe (FSSP) and a Johnson–Williams (J–W) cloud water probe mounted on the same pylon. Two particle imaging probes, PMS OAP-2D-P and OAP-2D-C, were carried on a pylon on the opposite wingtip. Airspeed and meteorological data were supplied by instruments mounted elsewhere on the wings and fuselage. Tower fly-bys conducted just prior to the project were used to calibrate static pressure and temperature sensors.

b. M-meter calibration

Flight segments at constant altitude and airspeed were used to estimate parameters Ω_a and K in (9). Values of $\Omega_a \approx 0.15$ and $K \approx 0.65$ were obtained. An accuracy of $\sim$0.000 87 ($\sim$0.6%) in $\Omega_a - \Omega$ is required to obtain M to an accuracy of 0.1 g m^{-3} from (9). Since flight data show that prototype Ω_a cannot be measured to this accuracy, accurate measurement of M is not expected from the prototype. Furthermore, in the field study described here, the air speed pitot and M-meter were mounted at different locations on the airplane [section 4c(1)] such that V and ω measurements were made in different air spaces and must include effects of slightly different airflows. Since Ω must be highly accurate because of the differencing required by (9), M accuracy would be compromised by this even if accurate Ω_a were available. Thus, our objective is to study relative changes, or trends, in M measurements, as compared with those of other instruments on the airplane, to verify that the M-meter concept is worthy of refinement.

c. Measurement accuracies of the other instruments

Of particular importance to interpretation of the data presented below are the following considerations:

1) Instruments were mounted at widely spaced sites on the airplane, and measurement uncertainties arise from this separation alone. Effects of instrument separation on accuracy of Ω were just discussed. Similarly, measurements made by hydrometeor instruments mounted on opposite wingtip pylons, separated by $\sim$14 m, can be expected to differ over small timescales due to natural small-scale spatial variations of hydrometeor concentrations (e.g., Jameson et al. 1998).

2) Volume sampling rates of the 2D-P and M-Meter are of the same order of magnitude ($\sim$0.16 m^3 s^{-1} for the 2D-P, $\sim$0.28 m^3 s^{-1} for the M-meter). They were on opposite wingtips, $\sim$14 m apart. The M-meter is specifically designed for response to hydrometeors in the size range sampled by the 2D-P, from $\sim$0.2 mm through several mm diameter, although the M-meter also responds to smaller and larger particles. Due to 2D array probe memory limitations, and the limitation that only one of the two 2D probes could dump its 4 kilobyte memory to the data acquisition system each second, images were obtained during only small fractions of a second during many of the seconds during which hydrometeor images were obtained. This further limited the volume sampled per second and increased the variability in M estimated from the imaging probes.

3) The 2D-C sampled at $\sim$0.005 m^3 s^{-1} and was on the same wingtip as the 2D-P, 14 m from the M-meter.

4) FSSP and J–W probes respond only to cloud droplets and sample at much smaller volume rates ($\sim$20 cm^3 s^{-1}) compared to the optical array probes. The FSSP was set to respond to cloud particles between 3- and 45-μm diameter. The J–W responds fully to particles in a distribution with mean volume diameter less than 30 μm, but incompletely to distributions of cloud particles with larger volume means (Spyers-Duran 1968). These two probes were on the same wingtip pylon as the M-meter. Due to the much higher number concentration of cloud droplets compared to precipitation hydrometeors, the cloud water probe readings were subject to much smaller sampling uncertainty than the precipitation water estimates derived from 2D-P and 2D-C image data. Davis and Lawson (1987) estimate accuracy of the 1-s sample FSSP and J–W cloud water concentrations to be $\pm$10%; although other sources suggest a more representative absolute accuracy for these instruments might be about $\pm$50%, depending on environmental conditions (e.g., Strapp and Schemenauer 1982; Gayet 1986; Baumgardner and Spowart 1990).

Detwiler et al. (1993) estimate that $\pm$15% accuracy of snow mass concentration can be achieved using large samples of image data ($\sim$100 hydrometeors, usually requiring two or more seconds of sampling time) from 2D-C and 2D-P probes if the mass versus size relationship for snow of the type sampled has been well established. For samples containing only a few hydrometeors, errors of up to 400% can occur. Mass can be determined from image data with greater accuracy for raindrops since drop density is known and the mass versus size relationship is simple. Accuracy for individual drops is a function of drop size (for a given probe resolution, larger drops can be sized relatively more accurately); a typical figure would be $\pm$10% for drizzle and rain drops within the optical sample volume. An estimate of mass concentration accurate to $\sim$10% could be achieved with a 1-s sample containing 20–40 valid images if the sample volume were precisely known. For samples higher in the melting layer that contain mixed-phase hydrometeors with a wide range of densities, poorer accuracy might be expected for both large and small samples.

We compute a size-dependent sample volume (Heymsfield and Parrish 1978). Uncertainties in sample volume and other probe operational characteristics contribute an additional uncertainty of several tens of percent in precipitation mass concentration estimates, (e.g., Heymsfield and Parrish 1978; Gayet et al. 1993).

d. The flight of 22 May 1986—Clear air results

A 5-min segment of level flight through clear air prior to the cloud penetration discussed in section 4e, is used

to illustrate field performance of the prototype M-meter under clear-air conditions. Figure 4a shows that altitude and compass heading during the segment were fairly constant. Figure 4b shows air speed and M-meter disk rotation rate versus time. Ranges of ordinate quantities on the graph are roughly proportional in magnitude such that they can be compared visually as shown. These results indicate high sensitivity of disk rotation to transient air speed changes, and support the findings of the sensitivity study discussed above.

Figure 4c shows disk rotation rate, ω, and normalized disk rotation rate, $\Omega = \Delta r\omega/(2V)$, plotted together versus time. Again, ranges of ordinate quantities on the graph are roughly proportional in magnitude such that they can be compared visually as shown. Notice that normalization removes much of the ''noisy'' variation in the disk rotation caused by airspeed transients. If airspeed were accurately measured very close to (in the same air space as) the M-meter, transient effects of turbulence and nonsteady flight would substantially cancel in Ω. This is critically important, since Ω is used in (9) to obtain M. [Note that normalizations of ω and ω_a to obtain Ω and Ω_a are independent, so that effects of the normalizations do not cancel in (9), as might be supposed at first glance.] Had V and ω been measured in the same air space we would expect the Ω curve in Fig. 4c to be even flatter and less noisy than shown. (Ideally, in clear air, $\Omega = \Omega_a$, and normalized rotation rate, Ω_a, in Fig. 4 would be a straight, horizontal line.)

FIG. 5. (a) 2D-P images for the period 1058:27–1058:54 UTC during a melting layer study conducted on 22 May 1986 near Boston. Vertical separator bars represent a scale of 6.4 mm. (b) 2D-C images obtained during the same time interval as the 2D-P images in (a). Image separators here represent a scale of 0.8 mm.

e. The flight of 22 May 1986—In cloud results

Data from a 15-min constant altitude flight leg just below a melting layer (temperature approximately +3°C) in a quasi-stratiform region of precipitation are used to illustrate in-cloud M-meter performance. Typical images from the two imaging probes taken during a 30-s segment of this leg are shown in Fig. 5. These hydrometeors appear to be mostly rain. The streak images indicate the presence of cloud and/or rain water collecting on probe tips and shedding periodically through the sample volume.

Hydrometer mass concentration, M, determined from image data from the two 2D probes and from the FSSP and J–W instruments are shown for the entire 15-min period in Fig. 6a–d. Estimates of M from the 2D probes were computed from 50 to 80 images. Since the computations assumed all-liquid hydrometeors, the estimates are upper limits. In most regions the total condensate is approximately equally divided between cloud water (droplets smaller than ~30-μm diameter) and drizzle/rain/graupel (particles larger than ~100-μm diameter). The exception is the region encountered two minutes before 1100 UTC, where the M represented in larger particles is estimated to be several times the M represented in cloud particles.

Also included in Fig. 6 are panels 6e–h, showing combined M from the FSSP (cloud water) and 2D-P (precipitation water) probes, M-meter M, true air speed V, and true air speed variance σ_v^2. Variance σ_v^2 is the root-mean-square deviation of V from mean V, where mean V for a particular time is the 5-s running mean centered on that time. Turbulence data are not available, so we take the liberty to use σ_v^2 as a crude proxy for turbulent kinetic energy on spatial scales of ~450 m and smaller. Comparison of Figs. 6g and 6h shows that peaks of higher σ_v^2 are associated with the significant V excursions.

There are three deep troughs (large negative excursions) of M-meter M: the first at 1059, the next just after 1100, and the third just after 1102 UTC. In all three cases, V exceeds 92 m s^{-1} (cf. Figs. 6f and 6g). Since at air speeds greater than ~92 m s^{-1} the prototype M-meter disk is known to stall, we infer that these troughs are the results of disk aerodynamic stall. They are not reactions to turbulence, airplane maneuvers, or other flight or cloud phenomena. Little hydrometeor M was encountered during these stalls, as indicated in Fig. 6e. By inspection of Fig. 6f, ignoring the three deepest troughs, it is apparent that the noise level of M calculated by (9) is about ± 0.2 g m^{-3}.

Figure 7a highlights the considerable correlation between M measured by the M-meter and M measured by the combination of FSSP and 2D-P probes. However,

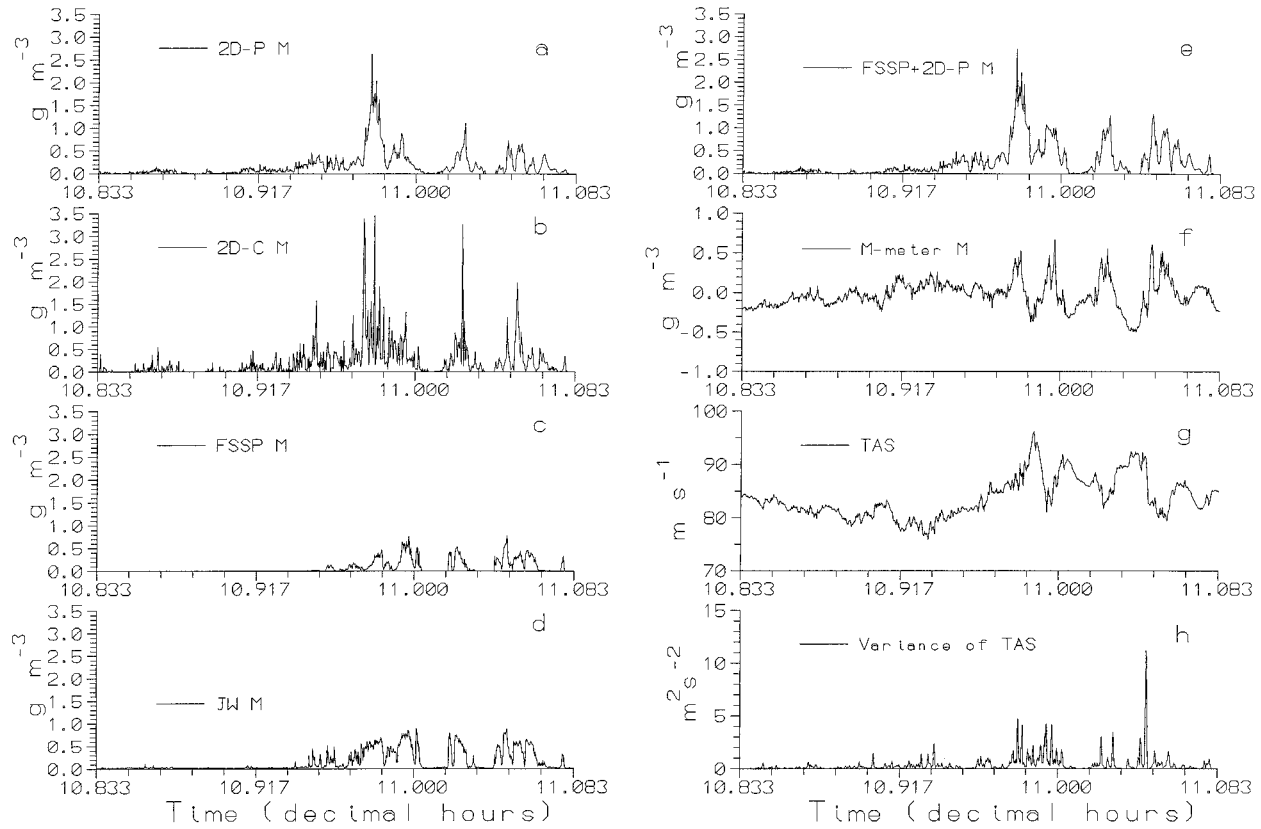

FIG. 6. Panels (a)–(d) show 2D-P, 2D-C, FSSP, and J–W values of M vs time for the 1050 to 1105 UTC in-cloud flight segment. Tics on the time axis are at 1-min intervals. Time is indicated in decimal hours. Panels (e)–(h) show combined M from the FSSP and 2D-P probes, M-meter M, true airspeed V, and true airspeed variance σ_v^2 (see text).

there is also apparent correlation of both M-meter M and FSSP + 2D-P M with as σ_v^2, as shown in Figs. 7b,c. Questions then arise as to relative correlations of M-meter M and FSSP + 2D-P M with turbulence, and further, as to how much, if any, of the calculated M-meter M actually is the result of sluggish disk reponse to high in-cloud turbulence, rather than response to hydrometeors. Figures 8a,b are scatterplots of FSSP + 2D-P M versus σ_v^2, and M-meter M versus σ_v^2. We see that the correlation coefficient, $r = 0.269$, of FSSP + 2D-P M with the turbulence proxy, is substantially higher than that of the M-meter M, $r = 0.181$. This rather clearly shows that M-meter M is no more a direct, spurious response to turbulence than is that of the optical instruments. Figure 8c shows the scatterplot of M-meter M versus FSSP + 2D-P M. The correlation coefficient of $r = 0.491$ between M-meter M and FSSP + 2D-P M is seen to be much higher than the correlations with turbulence. There can be little doubt that the M-meter responded to hydrometeors as predicted, and that the influence of turbulence on M-Meter M measurement was, at most, relatively minor.

We conclude that the M-meter M responses shown in Figs. 6 and 7, beyond the noise level of about ± 0.2 g m^{-3}, were caused by hydrometeors and aerodynamic disk stall. While, as expected, results are not as accurate as desired, the fundamental M-meter operating principles and response characteristics discussed in section 3 are supported by these field data.

The aerodynamic stall problem can be dealt with by improved design and by keeping air speed below the stall speed limit. Other problems, such as baseline drift and background noise level, can be reduced to acceptable levels by further development. Use of curved, rather than straight, vanes on the M-meter disk, and measurement of air speed at the same location as the M-meter on the airplane, would substantially reduce both of these problems. Use of curved vanes, which should have the shape of flow lines across the disk face, would remove the most questionable approximations and uncertainties involved in formulating the operation Eq. (9).

f. Other observations

All test flights were concentrated around the melting level, and good data were not obtained from extensive regions known to contain only rain. Rain and melting snow and graupel typically were found on legs below the melting level. Data from legs well above the melting

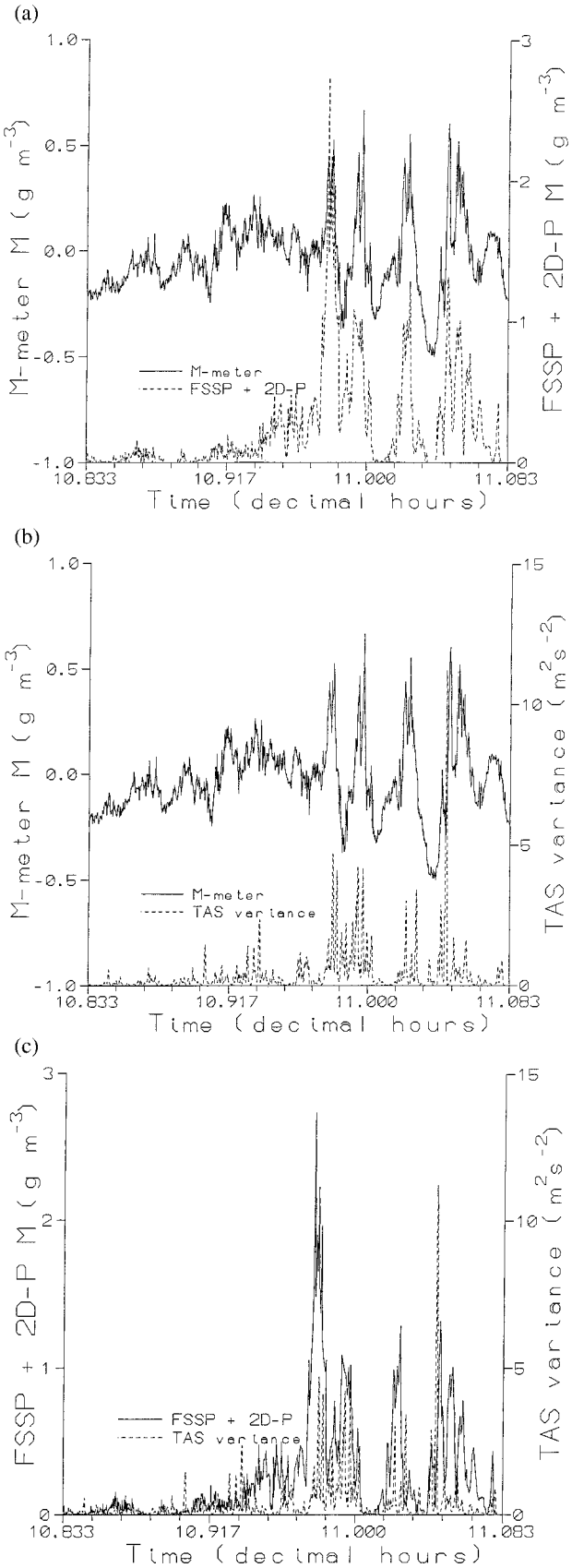

FIG. 7. Superimposed graphs showing selected parameters as a function of time: (a) M-meter M and FSSP + 2D-P M, (b) M-meter M and true airspeed variance σ_v^2, and (c) FSSP + 2D-P M and σ_v^2. Time interval and time axis tics are the same as in Fig. 6.

level, during which only snow and small amounts of cloud water were encountered, have been examined, but are not shown here. In these cases M estimated from the other probes is on the order of a few 0.1's g m^{-3}, and this is the approximate noise level in the M-meter M estimates. Thus the data do not establish clearly whether or not the M-meter responds as well to solid hydrometeors as it does to liquid and/or mixed phase hydrometeors.

While the prototype M-meter was in transit through a supercooled cloud near -10°C on a King Air airplane operated by the National Center for Atmospheric Research, during a program that was independent of the melting layer study discussed above, it was observed that icing dramatically changed the aerodynamic characteristics of the M-meter disk. In some cases icing led to increased rather than decreased rotation rate in the presence of cloud.

5. Further development

While preliminary results from the M-meter prototype are encouraging, a number of refinements in design are necessary. The most basic of these would ensure that more reliably constant and accurate values of parameters Ω_a and K be obtainable [see Eq. (9)]. Use of curved, instead of straight-slanted vanes (Fig. 1) is indicated by theoretical analysis to be potentially useful in this respect. In fact, the analysis indicates that with properly designed blades, Ω_a and K are fixed by design specifications, and can be determined accurately by both theory and measurement. A thorough laboratory/wind tunnel study of instrument design and response would be desirable. In this way, optimal vane design choices can be made in terms of curvature, height profile, and thickness. These experiments also would be used to determine optimum tradeoff balances between vane number, rotation speed and rotation response to variations in airspeed on the one hand, and response to hydrometeors on the other. Assessments of effects of bearing friction and boundary layer friction also are needed. During operation in the field, independent, highly accurate measurements of airspeed at a site very close to the M-meter are needed to minimize errors caused by disk rotation lag as it responds to turbulent flow fluctuations. This also would eliminate errors caused by distortions of airflow about the airplane. Response to frozen hydrometeors and effects of icing on vane aerodynamics must be studied, and an effective deicing or anti-icing capability must be added if reliable operation in supercooled cloud is to be achieved.

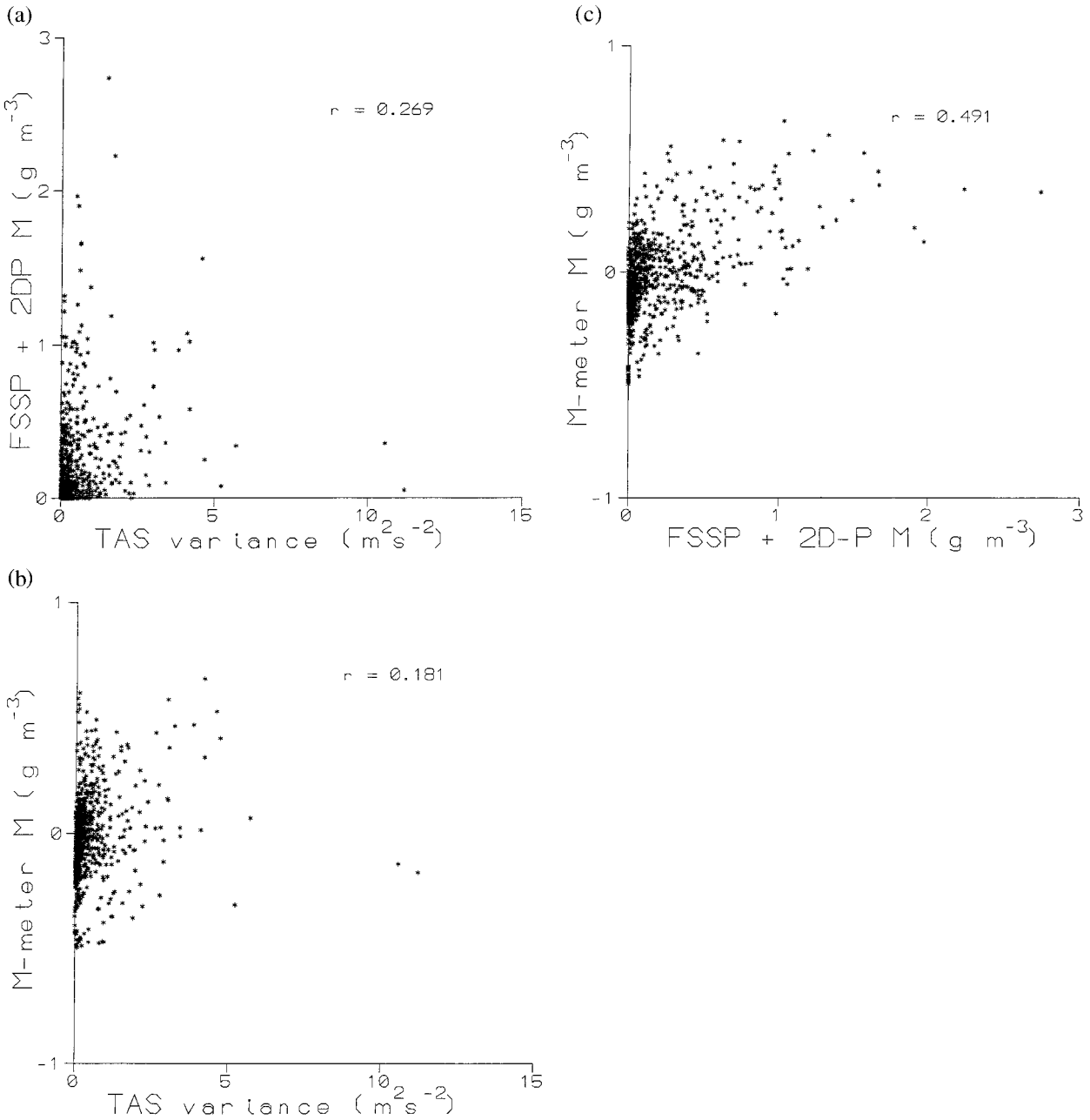

FIG. 8. Scatterplots and correlation coefficients: (a) FSSP + 2D-P M vs true air speed variance σ_v^2, (b) M-meter M vs σ_v^2, and (c) M-meter M vs FSSP + 2D-P M. Time interval and data are those of Figs. 6 and 7.

6. Conclusions

Plank's M-meter prototype is based on an aerodynamically driven, rotating disk. We predict equilibrium rotation rate to decrease in proportion to total mass concentration of cloud and precipitation hydrometeors encountered. The prototype instrument was field tested and was found to exhibit the predicted response. Qualitative measurements of mass concentration in clouds have been demonstrated. Rugged simplicity, relatively large volume sampling rate, and response to broad ranges of size spectra and types of hydrometeors augur well for its potential utility. Additional research and development, which is not planned by those presently involved, should achieve at least competitive, and perhaps superior, accuracy for in situ total condensed-phase water content measurement by this instrument.

Acknowledgments. The work reported here was done over more than 15 years with many interruptions. Until his passing in November 1995, Vern Plank was part of

this collaboration to design and improve his M-meter. Analyses, interpretations, and presentations of data and conclusions given here are solely those of the present authors. We gratefully acknowledge support and assistance from: Arnold Barnes, Morton Glass, and Dennis LaGross of the Phillips Laboratory (now U.S. Air Force Research Laboratory) at Hanscom AFB; Paul Lawson, then affiliated with the Colorado International Corporation and now with SPEC, Inc.; Darrel Baumgardner and the NCAR Research Aviation Facility; and Ken Hartman and Connie Crandall of the South Dakota School of Mines and Technology. The first author acknowledges partial support from cooperative agreements ATM-8620145, ATM-9104474, ATM-9401117, and ATM-9618569 between the National Science Foundation and the South Dakota School of Mines and Technology, and from a summer faculty research program at the Phillips Laboratory sponsored by the Air Force Office of Scientific Research.

REFERENCES

Baumgardner, D., and M. Spowart, 1990: Evaluation of the forward scattering spectrometer probe. Part III: Time response and laser inhomogeneity limitations. *J. Atmos. Oceanic Technol.,* **7,** 666–672.

Davis, L. G., and R. P. Lawson, 1987: Research and development to acquire and reduce melting layer cloud physics and evaluate a prototype M-Meter. AFGL Rep. TR-87-0161, 72 pp. [Available from Air Force Research Laboratory, Air Force Systems Command, United States Air Force, Hanscom Air Force Base, MA 01731-5000.]

Detwiler, A. G., N. C. Knight, and A. J. Heymsfield, 1993: Magnitude of error factors in estimates of snow-particle masses from images. *J. Appl. Meteor.,* **32,** 804–809.

Gayet, J. F., 1986: Calibration of Johnson-Williams and PMS ASSP probes in a wind tunnel. *J. Atmos. Oceanic Technol.,* **3,** 381–390.

——, P. R. A. Brown, and F. Albers, 1993: A comparison of in-cloud measurements obtained with six PMS 2D-C probes. *J. Atmos. Oceanic Technol.,* **10,** 180–194.

Heymsfield, A. J., and J. L. Parrish, 1978: Techniques employed in the processing of particle size spectra and state parameter data obtained with the T-28 aircraft platform. National Center for Atmospheric Research Rep. NCAR/TN-137&A, 78 pp. [Available from NCAR, P.O. Box 3000, Boulder, CO 80307-3000.]

Jameson, A. R., A. B. Kostinski, and R. A. Black, 1998: The texture of clouds. *J. Geophys. Res.,* **103,** 6211–6219.

Norment, H. G., 1982: Technical studies in support of the design of a cloud water content meter and hydrometeor spectrometer. AFGL Rep. TR-82-0188, 76 pp. [Available from Air Force Research Laboratory, Air Force Systems Command, United States Air Force, Hanscom Air Force Base, MA 01731-5000.]

Plank, V. G., 1986: The M-Meter (particulate mass sensor and spectrometer). Preprints, *Second Airborne Science Workshop,* Miami, FL, Rosentiel School of Marine and Atmospheric Science, University of Miami, 171–173.

Spyers-Duran, P. A., 1968: Comparative measurements of cloud liquid water using heated wire and cloud replicating devices. *J. Appl. Meteor.,* **3,** 450–460.

Strapp, J. W., and R. S. Schemenauer, 1982: Calibrations of Johnson-Williams liquid water content meters in a high-speed icing tunnel. *J. Appl. Meteor.,* **21,** 98–108.